J Cancer Res Clin Oncol (2011) 137:441–453
DOI 10.1007/s00432-010-0897-5

ORIGINAL PAPER

L-methionine-induced alterations in molecular signatures in MCF-7 and LNCaP cancer cells

Maximo A. Benavides · Dong Hu · Marie Kristine Baraoidan · Annette Bruno · Pan Du · Simon Lin · Wancai Yang · Kirby I. Bland · William E. Grizzle · Maarten C. Bosland

Received: 19 November 2009 / Accepted: 14 April 2010 / Published online: 9 May 2010

Abstract
Background Methionine inhibits proliferation of breast and prostate cancer cells. Here, we determined the influence of L-methionine on functional molecular signatures in these cell lines.
Methods MCF-7 and LNCaP cells were treated with L-methionine (5 mg/ml) for 72 h. Changes in molecular signatures of these cells were examined by microarray analysis of 15,814 probes in triplicate experiments.
Results In LNCaP cells, 325 genes were up-regulated by methionine, and 517 genes down-regulated. In MCF-7 cells, 86 genes were up-regulated and 135 genes down-regulated. Ninety-eight genes were regulated in the same direction by methionine in both cells lines, and five other genes were changed in expression in opposite directions.
Conclusion Several of the up-regulated genes encode proteins involved in cellular redox regulation, suggesting that methionine may enhance antioxidant mechanisms. Many of the down-regulated genes belong to protein kinase families that may be related to the anti-proliferative effects of methionine on breast and prostate cancer cells.

Keywords Methionine · Gene expression · Prostate cancer · Breast cancer · MCF-7 cells · LNCaP cells

Electronic supplementary material The online version of this article (doi:10.1007/s00432-010-0897-5) contains supplementary material, which is available to authorized users.

M. A. Benavides (✉) · D. Hu · W. Yang · M. C. Bosland (✉)
Department of Pathology, College of Medicine,
University of Illinois at Chicago, 840 South Wood Street,
Room 130 CSN, MC 847, Chicago, IL 60612, USA
e-mail: maxbenav@uic.edu

M. C. Bosland
e-mail: boslandm@uic.edu

M. K. Baraoidan · A. Bruno
DNA Service Laboratory, Research Resources Center,
University of Illinois at Chicago, Chicago, IL, USA

P. Du · S. Lin
Biomedical Informatics Center,
Robert H. Lurie Comprehensive Cancer Center,
Northwestern University, Chicago, IL, USA

K. I. Bland
Department of Surgery,
University of Alabama at Birmingham School of Medicine,
Birmingham, AL, USA

W. E. Grizzle
Department of Pathology,
University of Alabama at Birmingham School of Medicine,
Birmingham, AL, USA

Introduction

Recent investigations using new research tools have pointed to the potential of peptides as future therapeutic agents. Peptides possess a variety of potential clinical benefits, with applications in some of major categories of diseases, including cancer (Shrivastava et al. 2009; Vazquez et al. 2009). In addition to peptides, amino acid analogs are also potential candidates as new therapeutic agents. For example, our recent study (Benavides et al. 2007) has suggested that the amino acid methionine is a promising candidate anti-cancer compound, opening the prospect for development of methionine analogs as therapeutic agents.

Methionine is an essential amino acid that plays a key role in protein synthesis and in a number of other biochemical and cellular processes. Methionine is also implicated in DNA-methylation and protein-methylation by serving as the methyl-group donor, thereby serving an important role

in regulation of gene expression and protein functions. Furthermore, methionine is required for the biosynthesis of the polyamines spermine and spermidine, which are critically involved in a number of cellular activities including cell proliferation (Thomas and Thomas 2001).

One approach to identifying significant molecular events of malignant transformation and tumor progression and to characterizing both known and suspected oncogenic pathways is to establish molecular signatures using gene expression profiling (Sweet-Cordero et al. 2005). While such expression signatures of cancers are frequently confounded by the complexity of human tumors (Ji et al. 2003; Giustarini et al. 2004; Ji et al. 2004; Fagerholm et al. 2008), they can be more informative when applied to in vitro systems and to genetically modified animal models where experimental variables can be controlled (Huang et al. 2003).

We have previously shown that L-methionine possesses strong inhibitory effects on cell proliferation in both breast and prostate cancer cell lines and is associated with post-translational modification of the tumor suppressor gene p53 (Benavides et al. 2007; Benavides et al. 2010). In the present study, we have employed a global genomic approach to more comprehensively define gene signatures induced by L-methionine exposure of these cell lines and to understand the mechanisms that may underlie the methionine-mediated inhibitory effects on cell survival and cell cycle progression.

Materials and methods

Cell lines and cell culture

Wild-type p53-expressing LNCaP prostate and MCF-7 breast cancer cells were obtained from the American Type Culture Collection (ATCC; Manassas, VA). MCF-7 cells were cultured in Minimum Essential Medium (MEM; Eagle; Invitrogen, Grand Island, NY) containing 2 mM L-glutamine (Mediatech-Cellgro**,** Manassas, VA) 1.5 mg/L sodium bicarbonate, 0.1 mM non-essential amino acids, and 1 mM sodium pyruvate supplemented with 10% fetal bovine serum (FBS; vol/vol) (HyClone Lab Inc.; Logan, UT) and 10 mg/mL insulin (Pratt and Pollak 1993; Takahashi and Suzuki 1993). LNCaP (Horoszewicz et al. 1983) cells were cultured in RPMI 1640 media (Mediatech-Cellgro; Herndon, VA) supplemented with 10% FBS, 2 mM L-glutamine, antibiotic–antimycotic solution (1X; Mediatech-Cellgro), and MEM vitamin solution (1X; Mediatech-Cellgro). All cells were incubated at 37°C in a humidified atmosphere containing 5% CO_2.

Experimental design

Cells were seeded in 6-well plates at a concentration of 100,000 cells per well in 2 ml of media. After 48 h, cells were given fresh media to which L-methionine had been added at a concentration of 5 mg/ml or control media without additional thionine. After 72 h, cells were harvested. Three independent experiments were carried out for this study.

RNA isolation and microarray analysis

Cells were washed three times with ice-cold PBS and harvested using a trypsin. Total RNA was extracted using the RNase Mini Kit (Qiagen, Valencia, CA) according to the manufacturer's instructions. The concentration and purity of total RNA were determined spectrophotometrically at 260 and 280 nm. The quality of the RNA preparation was further evaluated by agarose gel electrophoresis. Biotin-labeled cRNA was generated from high-quality total RNA using the Illumina TotalPrep RNA Amplification kit (Ambion**,** Austin, TX). Briefly, 350 ng of total RNA with high 260/280 absorbance ratio (>1.8) (Gallagher 2001) and RIN number was reverse-transcribed with an oligo primer bearing T7 promoter. The first strands of cDNA, produced in the reaction, were used to make the second strands of cDNA. The purified second strands of cDNA along with biotin UTPs were used to generate biotinylated, antisense RNA of each mRNA in an in vitro transcription (IVT) reaction. The size distribution profiles for the labeled cRNA samples were evaluated by a bioanalyzer. Purified labeled cRNAs (1.5 μg) were hybridized to the Sentrix Human-6 v2 Expression Beadchip by overnight incubation at 55°C. Signals were developed with Streptavidin-Cy3. The Illumina BeadArray Reader was used to scan the chips.

Microarray data analysis

The Illumina Human WG6 V3 Expression BeadChip (Illumina: San Diego, California) was used to measure genome-wide gene expression levels. For quality control and statistical power consideration, samples from each cell line and treatment were analyzed in triplicate. The samples from the same cell lines (LNCaP and MCF-7) were laid out on the same slide (6 samples/slide) to avoid possible batch effects across slides. The Illumina Bead Array technology is based on randomly arranged beads, with each bead binding many (usually over 30) identical copies of a gene-specific probe. This redundant design yields high confidence calls and robust estimations. To take advantage of this unique feature of Illumina BeadArray, we used the Bioconductor lumi package (Du et al. 2007; Dalle-Donne et al. 2009) to preprocess Illumina data with default settings. Basically, each array was Variance-Stabilizing Transforms (VST) transformed and then followed by quantile normalization across all samples (Lin et al. 2008). Probes with intensity lower than or around background levels were filtered.

A total of 15,814 probes were used for further analysis. To identify differentially expressed genes, routines implemented in Illumina Bioconductor package (Smyth 2004) to fit linear models to the normalized expression values were applied. The variance used in the t-score calculation was corrected by an empirical Bayesian method (Smyth 2004) for better estimation relative to a small sample size. To control the effects of multiple testing and reduce false positives, *P*-values were further adjusted based on False Discovery Rate (FDR) (Benjamini and Hochberg 1995). We called genes with FDR-adjusted *P*-value <0.01 and a fold change >1.5 as differentially expressed genes.

Pathway analysis

Pathway Analysis was performed using Ingenuity Pathway Analysis (IPA 7.0) commercial software (www.Ingenuity.com). IPA information was extracted by Ingenuity from the scientific literature, including information about genes, drugs, chemicals, cellular and disease processes, and signaling and metabolic pathways. Expression data sets containing significant differentially expressed gene identifiers (Entrez Gene identifiers) and their corresponding expression values as fold changes were uploaded as a tab-delimited text file. Each gene identifier was mapped to its corresponding gene object in the Ingenuity Pathways Knowledge Base (IPKB). To start building networks, the application program queries the IPKB for interactions between focus genes and all other gene objects stored in the knowledge base and generates a set of networks. The program then computes a score for each network according to the fit of the network to the set of focus genes. The score indicates the likelihood of the focus genes in a given network being found together due to random chance. A score of larger than 2 indicates that there is a less than 1 in 100 chance that the focus genes were assembled randomly into a network due to random chance.

Quantitative reverse transcription–PCR (QRT–PCR)

Reverse transcription was carried out with a High Capacity cDNA Reverse Transcription Kit (Applied Biosystems, Foster City, CA) on the total RNA isolated from LNCaP and MCF-7 cells that had been cultured for 72 h with or without L-methionine (5 mg/ml) using the RNeasy kit from Qiagen. PCR conditions and sequence for each primer are shown in Table 1. PCR products were separated on a 1% agarose gel. Expression of a housekeeping gene, glyceraldehyde-3-phosphate dehydrogenase (GAPDH), was used to normalize the PCR. For real-time PCR, cDNA was mixed with primers and SYBR Green PCR Master Mix according to the manufacturer's instructions (Applied Biosystems). Real-time PCR was carried out by an ABI7900-HT

Table 1 Primer sequences used and results of confirmative quantitative RT–PCR analysis of 10 genes that were observed to be up-regulated by L-methionine

Gene symbol	Description of gene	LNCaP		MCF-7		Primer sequences	
		Fold change	*P* value	Fold change	*P* value	Forward	Reverse
LAMA3	Laminin, alpha 3	4.58	7.62E-04	4.96	4.19E-03	TCCCTATTTGCCAAGCCT	ACCGCTGTCCTGTAACT
AKR1C2	Aldo–keto reductase family 1, member C2	13.28	1.21E-03	3.57	1.45E-03	The primers used were from the Applied Biosystems Hs00912742_m1 protocol	
NQO1	NAD(P)H dehydrogenase, quinone 1	3.53	8.09E-06	2.44	9.16E-04	CAACCACGAGCCCAG	AGTGAGCCAGTACGATCAG
RBM4B	RNA binding motif protein 4B	2.57	1.65E-02	2.50	9.97E-03	GGTATGAACGGGAGCAGTAT	GCGGAGCAAGTTCTCAT
AFF3	AF4/FMR2 family, member 3	2.47	1.20E-02	5.64	1.99E-04	CAAGTTCAGCATCCCCAA	GTGGAAGCCAGGTCATCT
SH3BGRL	SH3 domain binding glutamic acid-rich protein-like	2.46	1.14E-03	2.26	4.23E-03	TGTTCCCAGGATGGTGAT	CTTCTAGGAAACCAAGCACA
GPX8	Glutathione peroxidase 8	2.00	4.00E-03	4.91	1.64E-03	CTCTGGAAAAGTATAAAGGCAAAG	TTGTGCAGTTCCTTCAGC
VAMP5	Vesicle-associated membrane protein 5 (myobrevin)	3.03	1.56E-03	1.78	8.84E-02	CCTCAGAGCAGTGACAGCAG	CCATTTGGCTTCTCCTTCAG
C8orf4	Chromosome 8 open reading frame 4	2.06	2.34E-03	3.44	7.84E-03	GGAAGATCCCCACATCGAT	TCAAAGATGTTGCCCACG
ATF3	Activating transcription factor 3	2.05	1.57E-03	3.08	1.48E-03	CATCACAAAGCCGAGGT	AGCTTCTCCGACTCTTTCTG

sequence detection system from Applied Biosystems for relative quantitation of mRNA levels, and the mRNA levels in methionine-exposed cells were plotted as fold increase compared with untreated samples. GAPDH was used for normalization ΔC_t values (target gene C_t minus GAPDH C_t) for each triplicate sample was averaged. $^{\Delta\Delta}C_t$ was calculated as previously described, and mRNA amplification was determined by the formula $2^{-\Delta\Delta}C_t$. For the real-time PCR of AKR1C2, we used the Taqman Gene Expression Assay from Applied Biosystems; the AKR1C2 Assay ID was Hs00912742_m1, and the GAPDH the assay ID was Hs99999905_m1.

Results

In this study, we compared the effects of treatment for 72 h with L-methionine at 5 mg/ml on gene expression in LNCaP prostate cancer cells and MCF-7 breast cancer cells, using as criteria a false discovery rate (FDR) *P*-value of greater than 0.01 and a change in expression of greater than 1.5-fold to select genes of interest in three independent experiments. Heatmaps were created to visualize the overall expression patterns of genes differentially expressed in LNCaP and MCF-7 cells treated with methionine or media without methionine added; the expression profile detected by each probe was first standardized with zero mean and one standard deviation. Clear differences in expression patterns were observed between LNCaP cells treated L-methionine and LNCaP controls and, to a lesser extent, between MCF-7 cells treated with methionine and MCF-7 cells given media without methionine added (Fig. 1).

The expression patterns of the majority of these genes were changed by methionine in the same direction in both cells lines. Volcano plots were created to indicate the strength of biological effects (fold change) versus the reproducibility of the result (*P*-value); each gene is represented as a dot in these plots (Fig. 2). Treatment with L-methionine

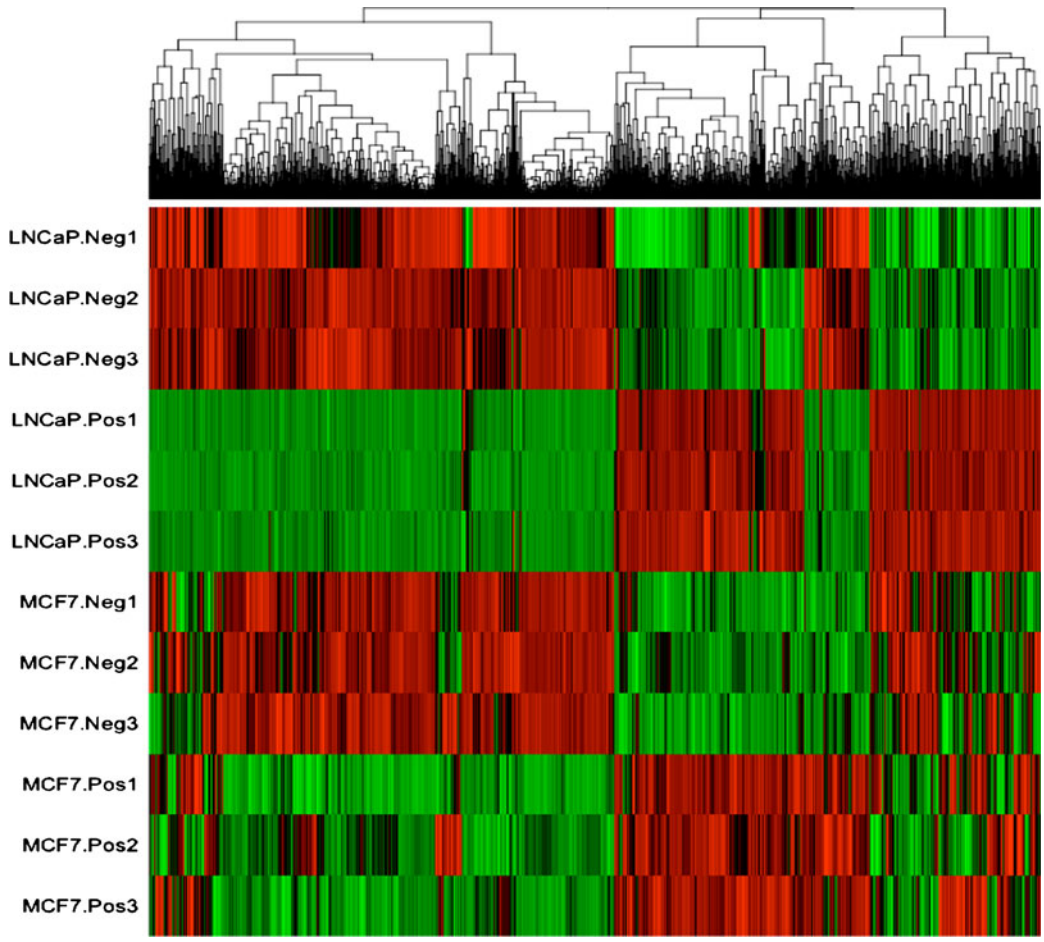

Fig. 1 Heatmap showing the overall expression patterns of all genes differentially expressed in either LNCaP and MCF-7 cells, comparing methionine-treated (*Pos*) and untreated control (*Neg*) cells in three independent replicate experiments (1, 2, and 3). Each row represents one sample and each column one probe. The expression profile of each probe was first standardized (zero mean and one standard deviation). The *red color* represents higher than average, *green color* represents lower than average, and *black* means close to the average

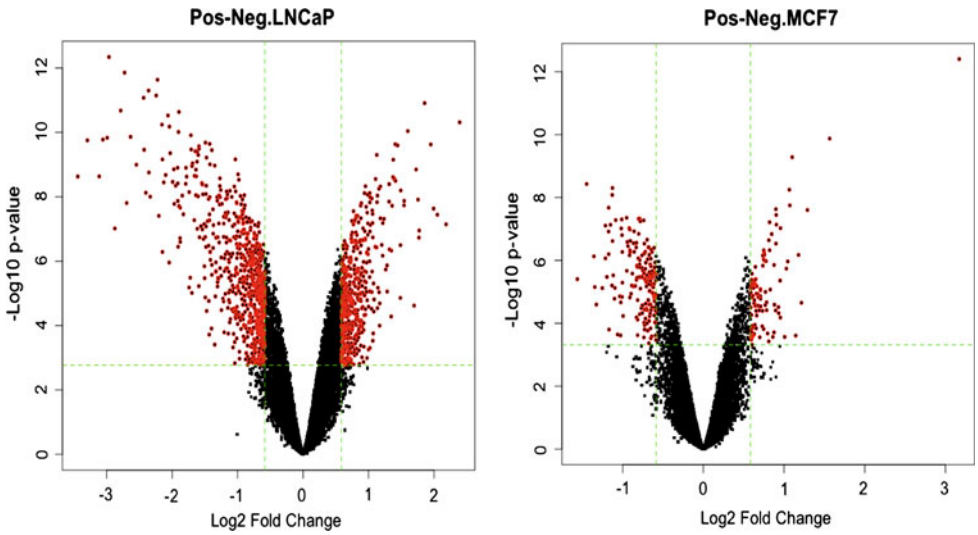

Fig. 2 Volcano plots in which each point represents the expression of a gene plotted as a function of fold change (Log2 (fold change), *x*-axis) after methionine exposure compared to untreated controls (*Pos–Neg*) and the statistical significance (−Log 10 (*P*-value), *y*-axis). *Vertical dotted lines* represent fold changes of ± 1.5, respectively. The *horizontal dotted line* represents an FDR of 0.01. The *red dots* represent differentially expressed genes with a FDR < 0.01 and fold change > 1.5

caused significant changes in expression of a total of 842 genes out of 15,814 probed in LNCaP cells, with 325 genes being up-regulated and 517 genes being down-regulated, while in MCF-7 cells, L-methionine treatment brought about a significant up-regulation of 86 genes and a down-regulation of 135 genes (Supplemental Tables 1 and 2). To explore the functional relevance of these findings and the observed commonalities and differences between the breast and prostate cancer cell lines, we first used Venn diagrams to identify overlapping gene signature responses to methionine between LNCaP and MCF-7 cells, again using the same criteria: FDR-adjusted *P*-value of <0.01 and a fold change of >1.5. This analysis revealed that 98 genes were modified by L-methionine treatment in the same direction in both cell lines, of which 10 genes were up-regulated and 88 genes were down-regulated (Table 2 and Fig. 3). In addition, the expression of the following five other genes was changed in opposite directions by L- methionine in LNCaP and MCF-7 cells (Fig. 3). H1 histone family member 0 (H1F0), Centromere Protein N (CENPN), and Acetyl-Coenzyme A Acetyltransferase 2 were up-regulated in LNCaP cells by 1.99 ($P < 0.001$), 1.65 ($P < 0.00005$), and 1.55-fold ($P < 0.00001$), respectively. In MCF-7 cells, these genes were down-regulated by 1.66 ($P < 0.0005$), 1.59 ($P < 0.0005$), and 1.57-fold ($P < 0.002$), respectively. In addition, Tumor Necrosis Factor Super Family member 2 (TNF-2) and Dehydrogenase/Reductase member 2 (DHRS2) were down-regulated in LNCaP by 1.75 and −1.52-fold, respectively ($P < 0.0005$), but they were up-regulated were up-regulated in MCF-7 cells by 1.51 ($P < 0.0005$), and 1.55-fold ($P < 0.001$), respectively. There was more variation in the response of MCF-7 cells to methionine in repeat experiments than for LNCaP cells (Fig. 3), which we cannot explain.

The 98 genes whose expression was modified by L-methionine treatment in the same direction in both cell lines were then analyzed using the data-mining tool IPA 7.0 (www.Ingenuity.com). Using this tool, we searched for functional relationships between differentially expressed genes identified in these microarray studies and those genes annotated in the Ingenuity knowledge base, the largest manually gene annotation database based on functional information available in published studies (www.Ingenuity.com). Six networks were identified that were defined as groups of two or more genes that are linked by a functional association, based on peer-reviewed published data.

Of these six functional network groups (summarized in Table 3), in group 1 (cancer, cell cycle and reproductive system diseases), only the LAMA3 gene was up-regulated, whereas 86% of genes were down-regulated and 11% was unchanged in their expression. In group 2 (cell cycle, cell assembly/organization, DNA replication, recombination and repair), only GPX8 was up-regulated, while 57% of genes were down-regulated and 40% remained unchanged. In group 3 (DNA replication, recombination and repair, cancer, and gastrointestinal disease), two genes (NQO1 and C8ORF4) were up-regulated. Fifty-one percent of the remaining genes were down-regulated, and 43% genes were unchanged. In group 4 (cancer, gastrointestinal disease and cell cycle), two genes (ATF3 and SH3BGRL) were up-regulated. In this group, 46% of genes were down-regulated, and 49% genes were unchanged. In group 5 (cancer, gastrointestinal disease, genetic disorders), four genes (AFF3, AKR1C2, RBM4B, and VAMP5) were up-regulated. Thirty-four percent of genes in this group were down-regulated, and 54% genes were unchanged. Of the two genes in group 6 (cell death, neurological diseases, nervous system development and function), the FBXO38 gene was down-regulated, and KLF7 was unchanged.

To confirm the expression of key genes differentially regulated by the L-methionine treatment, the expression of the ten genes that were up-regulated (e.g., AFF3, AKR1C2,

Table 2 Comparisons between methionine-treated and control LNCaP and MCF-7 cells revealing that the expression of 98 genes was changed in the same direction in both cell lines based on the following criteria: a false discovery rate (FDR)–adjusted *P*-value <0.01 and a fold change >1.5

No.	Probe.NuID	EntrezID	Symbol	Description	LNCaP			MCF-7		
					Fold change	*P* value	FDR	Fold change	*P* value	FDR
1	rkdrpLRTAEETXkXoHo	3909	LAMA3	Laminin, alpha 3	2.60	7.05E-10	2.86E-07	1.67	6.96E-07	1.72E-04
2	rXn6YfSwnEnCVNpaAI	1646	AKR1C2	Aldo–keto reductase family 1, member C2 (dihydrodiol dehydrogenase 2; bile acid binding protein; 3-alpha hydroxysteroid dehydrogenase, type III)	2.32	6.75E-07	3.10E-05	1.52	4.81E-04	9.93E-03
3	upHrr.53YSzUQyeGno	1728	NQO1	NAD(P)H dehydrogenase, quinone 1	2.30	3.13E-07	1.79E-05	1.52	2.58E-04	6.60E-03
4	9Vyi_DX3V5cXkk3X9U	83759	RBM4B	RNA binding motif protein 4B	2.08	2.66E-08	3.11E-06	1.69	9.95E-07	2.13E-04
5	osj1QiH8ktFJfDk7Eo	3899	AFF3	AF4/FMR2 family, member 3	1.88	2.65E-05	4.35E-04	1.62	2.78E-04	6.94E-03
6	Nd8wBK_mNP1Qj6.V_I	6451	SH3BGRL	SH3 domain binding glutamic acid-rich protein-like	1.83	9.81E-06	2.16E-04	1.57	1.45E-04	4.41E-03
7	35QRHIUd.o9CJHuzh4	493869	GPX8	Glutathione peroxidase 8	1.81	6.42E-06	1.59E-04	1.78	8.42E-06	6.72E-04
8	3TXj7nnrbf3V0iS4SQ	10791	VAMP5	Vesicle-associated membrane protein 5 (myobrevin)	1.77	1.53E-07	1.08E-05	1.51	4.33E-06	4.37E-04
9	0jp6I4T81KtH_0pXKE	56892	C8orf4	Chromosome 8 open reading frame 4	1.56	5.44E-04	4.21E-03	1.68	1.52E-04	4.57E-03
10	HdUm8EQDU6ks46Std4	467	ATF3	Activating transcription factor 3	1.53	4.04E-05	5.92E-04	1.60	1.45E-05	9.57E-04
11	ccp.nyzTtTv19F0uic	51203	NUSAP1	Nucleolar and spindle associated protein 1	−9.80	1.76E-10	1.39E-07	−1.99	5.85E-05	2.29E-03
12	iKKgVb_bmVB1QukAKA	9768	KIAA0101	KIAA0101	−8.32	1.66E-10	1.39E-07	−2.03	2.15E-05	1.25E-03
13	HClLklAJJdNRQpNZ4I	991	CDC20	Cell division cycle 20 homolog (*S. cerevisiae*)	−7.95	1.46E-10	1.29E-07	−2.29	3.36E-06	3.90E-04
14	x.Sd_F7Vd6eXeLeDdU	7153	TOP2A	Topoisomerase (DNA) II alpha 170 kDa	−7.80	4.54E-13	7.18E-09	−1.67	2.62E-06	3.55E-04
15	clyu1_J4FkeCB37XR4	113130	CDCA5	Cell division cycle associated 5	−6.90	2.09E-11	4.05E-08	−1.59	8.50E-05	3.01E-03
16	rSTjV0ngdAJbQIX5dU	9133	CCNB2	Cyclin B2	−6.62	1.39E-12	1.10E-08	−2.26	2.10E-08	3.58E-05
17	ZqR1Qw4LulILoN.Eoc	983	CDC2	Cell division cycle 2, G1 to S and G2 to M	−6.20	1.37E-10	1.27E-07	−2.01	5.12E-06	4.97E-04
18	o.fSL_0zHn7TeTx0k	3161	HMMR	Hyaluronan-mediated motility receptor (RHAMM)	−5.84	1.01E-09	3.71E-07	−2.19	6.29E-06	5.60E-04
19	BngJ4o2iQv3oZHz9XU	8318	CDC45L	CDC45 cell division cycle 45-like (*S. cerevisiae*)	−5.40	8.35E-12	2.20E-08	−1.77	1.45E-06	2.69E-04
20	rUvfXhFo6ufqBb_JfM	29128	UHRF1	Ubiquitin-like with PHD and ring finger domains 1	−5.38	3.46E-10	1.88E-07	−1.73	5.13E-05	2.12E-03
21	N4TSXn31Xeaf0eeL94	7083	TK1	Thymidine kinase 1, soluble	−5.28	7.51E-09	1.40E-06	−2.38	7.60E-06	6.23E-04
22	Z46PfU15aOLuruMSXE	9833	MELK	Maternal embryonic leucine zipper kinase	−5.13	5.03E-12	1.99E-08	−1.87	2.40E-07	1.06E-04
23	iTtHHqiu9edyfUY4pk	9055	PRC1	Protein regulator of cytokinesis 1	−4.67	2.30E-12	1.21E-08	−1.66	6.04E-07	1.67E-04
24	QkXgJ9dhN7wwJbKV_0	332	BIRC5	Baculoviral IAP repeat-containing 5	−4.28	2.10E-09	6.27E-07	−1.88	1.51E-05	9.72E-04
25	Th3rxI_343fo3XSN.o	55872	PBK	PDZ binding kinase	−4.18	2.97E-11	4.70E-08	−1.81	5.33E-07	1.55E-04
26	xX7dOhfRSFxdAkUSTk	890	CCNA2	Cyclin A2	−4.12	6.59E-11	8.02E-08	−1.88	5.44E-07	1.55E-04
27	6e.BIM4nt7T8XH39Uc	4751	NEK2	NIMA (never in mitosis gene a)-related kinase 2	−4.08	4.40E-10	2.11E-07	−1.62	3.75E-05	1.72E-03
28	rjki1Tu13jcC_Tr63 g	11339	OIP5	Opa interacting protein 5	−3.98	3.45E-09	8.39E-07	−1.57	2.96E-04	7.20E-03
29	ogf9RSSoFUIk1DIJ7 k	4001	LMNB1	Lamin B1	−3.85	4.54E-09	9.83E-07	−1.66	1.14E-04	3.74E-03
30	TqCLahRL88UPeKC1l8	4085	MAD2L1	MAD2 mitotic arrest deficient-like 1 (yeast)	−3.77	3.85E-09	8.96E-07	−1.56	2.60E-04	6.62E-03

Table 2 continued

No.	Probe.NuID	EntrezID	Symbol	Description	LNCaP			MCF-7		
					Fold change	*P* value	FDR	Fold change	*P* value	FDR
31	6W70h16.fUp8S6E00k	81610	FAM83D	Family with sequence similarity 83, member D	−3.73	9.65E-11	1.02E-07	−2.12	5.22E-08	4.66E-05
32	fgbdYtXQd3Gf5dQrgU	3833	KIFC1	Kinesin family member C1	−3.72	2.30E-11	4.05E-08	−2.19	8.30E-09	1.88E-05
33	NLdHHg5Rffj0UrcB5I	9787	DLGAP5	Disks, large (Drosophila) homolog-associated protein 5	−3.67	2.17E-08	2.62E-06	−2.01	1.45E-05	9.57E-04
34	NjXGdGm9 V.HQN6 l.6Q	10112	KIF20A	Kinesin family member 20A	−3.59	9.20E-09	1.52E-06	−2.32	8.58E-07	1.97E-04
35	QLR0VHu.euUKd_KlUc	54478	FAM64A	Family with sequence similarity 64, member A	−3.55	3.49E-08	3.78E-06	−2.14	7.51E-06	6.18E-04
36	i13nKFKuP0JSoJB6hU	55723	ASF1B	ASF1 anti-silencing function 1 homolog B (*S. cerevisiae*)	−3.43	2.37E-09	6.45E-07	−1.93	2.14E-06	3.20E-04
37	QL7MM5_wKeKuJ7N6OU	55388	MCM10	Minichromosome maintenance complex component 10	−3.28	1.22E-10	1.21E-07	−1.58	4.43E-06	4.41E-04
38	9d5S3L96kr9e7Sz1V0	83879	CDCA7	Cell division cycle associated 7	−3.27	3.39E-10	1.88E-07	−1.64	4.30E-06	4.37E-04
39	TWl6.Zetu384kU7CXU	1870	E2F2	E2F transcription factor 2	−3.24	1.10E-09	3.86E-07	−1.60	1.82E-05	1.12E-03
40	HfpVTFVBftS6JUH3Ao	29127	RACGAP1	Rac GTPase activating protein 1	−3.22	9.19E-10	3.54E-07	−1.73	3.39E-06	3.90E-04
41	ortS6TUiAkXzi6CD_g	8836	GGH	Gamma-glutamyl hydrolase (conjugase, folylpolygammaglutamyl hydrolase)	−3.15	2.23E-09	6.45E-07	−2.01	5.38E-07	1.55E-04
42	uR6JSuH11_bi4qRKDc	25886	WDR51A	WD repeat domain 51A	−3.13	3.83E-10	1.95E-07	−1.68	2.08E-06	3.19E-04
43	0p.q69Q_uiIJ3ikbTk	4172	MCM3	Minichromosome maintenance complex component 3	−3.11	8.96E-09	1.52E-06	−1.59	8.40E-05	3.00E-03
44	0nu9VB3veZGASze.ik	55165	CEP55	Centrosomal protein 55 kDa	−3.07	8.07E-10	3.19E-07	−1.91	3.49E-07	1.31E-04
45	xp6 k.U0zIXeV9Isl0U	1058	CENPA	Centromere protein A	−3.07	4.03E-10	1.99E-07	−1.75	8.58E-07	1.97E-04
46	3ieeV36bi_bPSnn.nk	4171	MCM2	Minichromosome maintenance complex component 2	−3.04	9.66E-09	1.56E-06	−1.82	6.66E-06	5.78E-04
47	o7h_frpdPU7uXuXqk4	55143	CDCA8	Cell division cycle associated 8	−3.03	5.02E-10	2.27E-07	−1.69	1.74E-06	2.86E-04
48	3ZI6Kh14TJSee4DDoI	1033	CDKN3	Cyclin-dependent kinase inhibitor 3	−2.99	1.81E-07	1.22E-05	−2.05	1.39E-05	9.38E-04
49	Teq_16d6oiIaJfyxJw	11004	KIF2C	Kinesin family member 2C	−2.92	3.77E-09	8.90E-07	−1.59	2.52E-05	1.36E-03
50	NRBiFzZZNtCuhcC9Vk	9212	AURKB	Aurora kinase B	−2.90	1.03E-07	8.02E-06	−2.17	2.97E-06	3.81E-04
51	ooKJT36B6GH3gB6KGI	83461	CDCA3	Cell division cycle associated 3	−2.89	8.40E-09	1.48E-06	−2.18	2.42E-07	1.06E-04
52	BepQfvreD3XB1P_Ank	7272	TTK	TTK protein kinase	−2.82	1.78E-07	1.22E-05	−1.78	6.50E-05	2.48E-03
53	Wg57u3taRVrKXj6v3I	6790	AURKA	Aurora kinase A	−2.81	2.07E-10	1.56E-07	−2.18	4.98E-09	1.49E-05
54	BI90n1UokIXeJWUJmk	4176	MCM7	Minichromosome maintenance complex component 7	−2.80	8.22E-09	1.48E-06	−1.78	4.13E-06	4.29E-04
55	Knknb10Xk4iCDgiPSI	10874	NMU	Neuromedin U	−2.79	8.32E-08	6.64E-06	−1.66	9.58E-05	3.28E-03
56	QXnojsD_U4fXooSSTo	11130	ZWINT	ZW10 interactor	−2.69	2.27E-10	1.56E-07	−1.74	1.43E-07	7.42E-05

Table 2 continued

No.	Probe.NuID	EntrezID	Symbol	Description	LNCaP			MCF-7		
					Fold change	*P* value	FDR	Fold change	*P* value	FDR
57	lKKIuwl4K3.yCn10.o	699	BUB1	BUB1 budding uninhibited by benzimidazoles 1 homolog (yeast)	−2.69	1.03E-08	1.58E-06	−1.77	3.59E-06	4.03E-04
58	liCOpICeiVei_nu3u8	2237	FEN1	Flap structure-specific endonuclease 1	−2.68	9.82E-10	3.70E-07	−1.59	3.32E-06	3.90E-04
59	3f6sV8hd49wtA5A6vA	55789	DEPDC1B	DEP domain containing 1B	−2.67	5.18E-07	2.54E-05	−1.67	2.82E-04	7.01E-03
60	uOq6EEW0haiFKknfRI	55355	HJURP	Holliday junction recognition protein	−2.63	3.56E-10	1.88E-07	−1.65	5.31E-07	1.55E-04
61	cYOko5Xu.T1L6955VU	10024	TROAP	Trophinin associated protein (tastin)	−2.59	1.40E-07	1.00E-05	−1.86	1.14E-05	8.41E-04
62	9pY7gGgiYFKckAif30	84057	MND1	Meiotic nuclear divisions 1 homolog (*S. cerevisiae*)	−2.49	1.02E-08	1.58E-06	−1.51	3.93E-05	1.76E-03
63	NH1MoTHk7CULTog3nk	891	CCNB1	Cyclin B1	−2.43	9.25E-09	1.52E-06	−1.73	1.64E-06	2.81E-04
64	BSXeHuXs3VA91HY9R4	22974	TPX2	TPX2, microtubule-associated, homolog (*Xenopus laevis*)	−2.42	4.60E-09	9.83E-07	−1.62	2.99E-06	3.81E-04
65	3.0uJuuHkivLnuAJ6k	26047	CNTNAP2	Contactin-associated protein-like 2	−2.41	2.67E-09	7.03E-07	−1.58	3.31E-06	3.90E-04
66	xWRvd5Vv35VLuv5Pt0	3925	STMN1	Stathmin 1/oncoprotein 18	−2.41	1.02E-08	1.58E-06	−1.92	2.60E-07	1.11E-04
67	ioJIoIo4AO5S4n4tfo	10403	NDC80	NDC80 homolog, kinetochore complex component (*S. cerevisiae*)	−2.39	6.15E-09	1.23E-06	−1.51	1.57E-05	1.00E-03
68	lazqZV5PnqO.eVGv_8	9319	TRIP13	Thyroid hormone receptor interactor 13	−2.36	1.66E-08	2.15E-06	−2.01	1.57E-07	7.77E-05
69	cUiuQDkokiLuj3SUrU	1062	CENPE	Centromere protein E, 312 kDa	−2.32	4.15E-08	4.26E-06	−1.56	3.08E-05	1.53E-03
70	WlF1W79QtJ.XkIIDXo	2305	FOXM1	Forkhead box M1	−2.25	3.66E-08	3.89E-06	−1.70	3.34E-06	3.90E-04
71	9V8od6z.43pBTP3oL4	3832	KIF11	Kinesin family member 11	−2.24	6.82E-09	1.30E-06	−1.89	9.43E-08	5.84E-05
72	3aVeAhBJ1f3n2hFHQE	116028	C16orf75	Chromosome 16 open reading frame 75	−2.23	5.15E-07	2.54E-05	−1.76	1.83E-05	1.12E-03
73	irShFNehxEdZiuhGtw	4521	NUDT1	Nudix (nucleoside diphosphate linked moiety X)-type motif 1	−2.19	9.07E-07	3.87E-05	−2.26	6.33E-07	1.72E-04
74	K63vX_n936K6tkkUjo	8914	TIMELESS	Timeless homolog (Drosophila)	−2.19	5.23E-08	4.98E-06	−1.50	4.06E-05	1.78E-03
75	Zn56RLL8V7ze79MOqk	9928	KIF14	Kinesin family member 14	−2.14	7.22E-07	3.28E-05	−1.85	6.31E-06	5.60E-04
76	rXg2T3ceh3pefoiukk	84722	PSRC1	Proline/serine-rich coiled-coil 1	−2.10	8.10E-08	6.56E-06	−1.88	4.77E-07	1.51E-04
77	HXfUJXm1JibRJEF5AA	84823	LMNB2	Lamin B2	−2.04	1.79E-06	6.39E-05	−1.50	3.40E-04	7.79E-03
78	fieOjriigofChJO3qg	1515	CTSL2	Cathepsin L2	−2.02	2.93E-07	1.71E-05	−2.22	7.35E-08	5.28E-05
79	9jpCddAlL7AMrVeXrE	26271	FBXO5	F-box protein 5	−1.99	1.99E-09	6.07E-07	−1.67	5.30E-08	4.66E-05
80	Kbi2l5Tv1O5T98Vfso	81691	LOC81691	Exonuclease NEF-sp	−1.95	1.72E-07	1.19E-05	−1.52	1.95E-05	1.16E-03
81	lRA1XkJz0Drjoxn6T0	259266	ASPM	Asp (abnormal spindle) homolog, microcephaly associated (Drosophila)	−1.95	3.62E-06	1.03E-04	−1.70	3.28E-05	1.59E-03
82	BslSRJ9.skdYOv6Fuk	995	CDC25C	Cell division cycle 25 homolog C (*S. pombe*)	−1.91	2.74E-08	3.19E-06	−1.53	2.51E-06	3.49E-04
83	lo7qXyXUrUhxx3O91I	24137	KIF4A	Kinesin family member 4A	−1.90	3.50E-08	3.78E-06	−1.57	1.52E-06	2.76E-04
84	B91yrztS_q.8KSRIeU	7374	UNG	Uracil-DNA glycosylase	−1.89	2.92E-08	3.32E-06	−1.52	2.38E-06	3.39E-04

Table 2 continued

No.	Probe.NuID	EntrezID	Symbol	Description	LNCaP			MCF-7		
					Fold change	*P* value	FDR	Fold change	*P* value	FDR
85	BSeoXozSTRkQVCZACU	9493	KIF23	Kinesin family member 23	−1.88	6.28E-06	1.56E-04	−1.57	1.44E-04	4.41E-03
86	Nnp0VyCVB1B3lH9xCQ	55771	PRR11	Proline rich 11	−1.88	6.21E-08	5.51E-06	−1.81	1.19E-07	6.60E-05
87	3Z6l7r4jC0UnGgr94Y	54892	NCAPG2	Non-SMC condensin II complex, subunit G2	−1.87	3.29E-07	1.83E-05	−1.73	1.33E-06	2.54E-04
88	lokghwIgYonhSjeYYU	10460	TACC3	Transforming, acidic coiled-coil containing protein 3	−1.84	3.17E-07	1.81E-05	−1.53	1.39E-05	9.38E-04
89	umjOoR8Axx_nVCNijg	5111	PCNA	Proliferating cell nuclear antigen	−1.81	3.07E-07	1.77E-05	−1.82	2.82E-07	1.13E-04
90	Q5K_yf.jqcdMS8j.Ek	3148	HMGB2	High-mobility group box 2	−1.81	1.37E-06	5.19E-05	−1.89	6.84E-07	1.72E-04
91	ZVChN4dVxd.O3lS7Po	5427	POLE2	Polymerase (DNA directed), epsilon 2 (p59 subunit)	−1.80	5.61E-07	2.69E-05	−1.66	2.48E-06	3.47E-04
92	91V_0SAUqHfSj_I6X4	27235	COQ2	Coenzyme Q2 homolog, prenyltransferase (yeast)	−1.79	5.09E-07	2.54E-05	−1.53	1.33E-05	9.30E-04
93	Tk14qaIFIIY4p15AKw	55646	LYAR	Ly1 antibody reactive homolog (mouse)	−1.71	8.60E-06	1.97E-04	−1.52	9.30E-05	3.22E-03
94	fkoPdfCooiQkrulUn0	83543	C9orf58	Chromosome 9 open reading frame 58	−1.66	8.09E-07	3.55E-05	−1.56	3.56E-06	4.02E-04
95	xij3cugh0gPpG7ngoE	51053	GMNN	Geminin, DNA replication inhibitor	−1.65	5.43E-06	1.41E-04	−1.69	3.40E-06	3.90E-04
96	fIAk8VP_aUL1YYinoU	57706	DENND1A	DENN/MADD domain containing 1A	−1.60	2.88E-06	8.88E-05	−1.54	7.13E-06	6.03E-04
97	ckKhzgu0jLlXTfipck	57405	SPC25	SPC25, NDC80 kinetochore complex component, homolog (*S. cerevisiae*)	−1.54	2.50E-06	7.98E-05	−1.58	1.33E-06	2.54E-04
98	QUSofik5L6itena.nM	81545	FBXO38	F-box protein 38	−1.52	5.77E-05	7.73E-04	−1.53	5.62E-05	2.24E-03

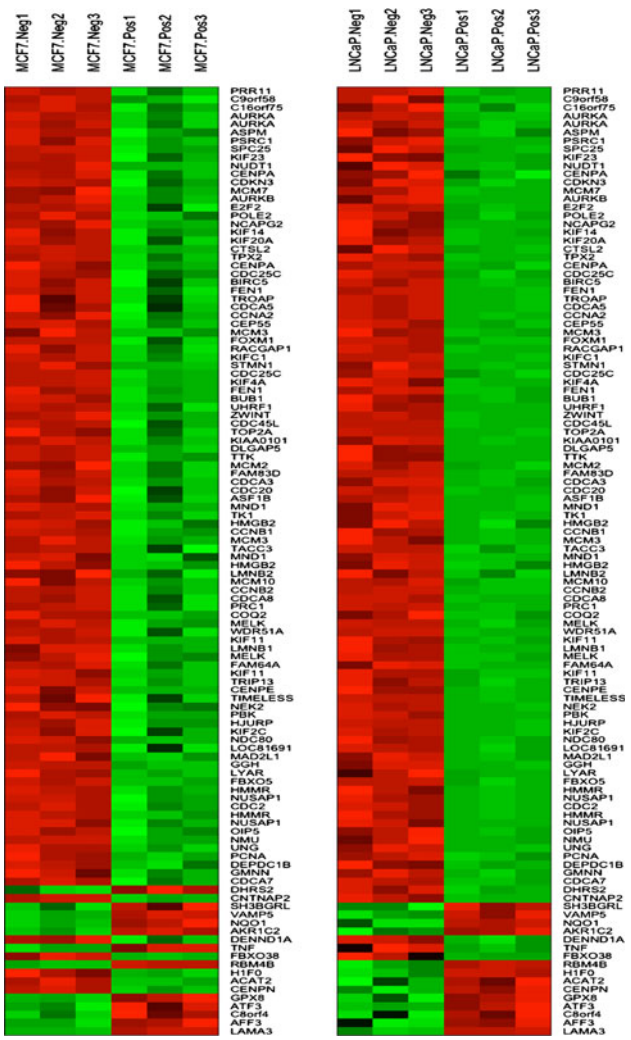

Fig. 3 Heatmap of genes the expression of which was altered by L-methionine treatment in both LNCaP and MCF-7 cells, comparing methionine-treated (*Pos*) and untreated control (*Neg*) cells in three independent experiments (1, 2, and 3). Of these 103 genes, 98 were regulated in the same direction by this treatment, with 10 genes up-regulated and 88 genes down-regulated in both cancer cell lines. The expression of five other genes was changed in opposite directions in the two cell lines (see text of results)

ATF3, C8ORF4, GPX8, LAMA3, RBM4B, NQO1, SH3BGRL, and VAMP5) was further assessed by real-time RT–PCR analysis, and their expression was compared with the changes in expression patterns detected by the microarray analysis. There was strong induction of the mRNA expression of each of these genes after treatment with L-methionine using both microarray analysis and real-time RT–PCR (Table 1).

Discussion

In the present study, we identified, using microarray analysis, 98 genes whose expression was increased (10 genes) or decreased (88 genes) by treatment with L-methionine for 72 h at the non-apoptosis-inducing concentration of 5 mg/ml in both prostate cancer LNCaP cells and breast cancer MCF-7 cells. The expression of five genes was modified in opposite directions in these two cell lines. The dysregulation of these 98 genes in both breast and prostate cancer cells suggests that the affected genes are potential common regulatory targets of methionine and, possibly, methionine analogs. On the other hand, there were considerable differences between these two cell lines in the effect of methionine. L-methionine caused significant expression changes of 842 genes in LNCaP cells, whereas only 221 genes were affected in MCF-7 cells. It is not clear why this difference occurred, but of note, MCF-7 cells are also less sensitive to inhibition of cell proliferation caused by methionine (Benavides et al. 2010).

Three of the genes up-regulated by L-methionine in both cell lines, NAD (P)H:quinone oxidoreductase (NQO1), SH3BGRL (SH3BGRL), and glutathione peroxidase 8 (GPX8), are associated with changes in cellular thiol redox balance and are involved cellular defense against oxidative stress (Forthoffer et al. 2002; Mazzocco et al. 2002; Santa-Cruz et al. 2004; Toppo et al. 2008; Yin et al. 2005). These findings suggests that L-methionine may induce antioxidant effects and consequently regulate the cellular pool of glutathione, which is required for maintaining the reduced state of cellular protein thiol groups (Metayer et al. 2008). It is conceivable that the induction of these antioxidant-related genes by L-methionine may bring about increased antioxidant capacity in cancer cells. Of note, methionine also serves as a precursor of glutathione, a tripeptide that is a regulator of intracellular redox homeostasis, which by reducing a sulfhydryl-containing reactive oxygen species (ROS) safeguards cells from oxidative stress (Anderson 1998). NQO1 serves as a quinone reductase in connection with conjugation reactions of hydroquinones involved in detoxification pathways in addition to other functions (Bello et al. 2001). Reduced expression of NQO1 has been detected in breast cancer cells and is believed to be a strong prognostic and predictive factor in breast cancer (Fagerholm et al. 2008). SH3BGR has been suggested to represent a novel class of thioredoxin fold proteins belonging to the thioredoxin superfamily (Yin et al. 2005). GPX8 reduces hydrogen peroxide by transferring the energy of the reactive peroxides to a glutathione (Toppo et al. 2008).

Interestingly, also up-regulated was aldo-keto reductase family 1, member C2 (AKR1C2), which catalyzes the inactivation of the potent androgen 5-alpha-dihydrotestosterone (5-alpha-DHT) to 5-alpha-androstane-3-alpha, 17-beta-diol (3-alpha-diol), thereby possibly reducing androgen activity in LNCaP cells (Lou et al. 2006). The expression of AKR1C2 is known to be reduced in both prostate cancer and breast cancer cells (Ji et al. 2003, 2004).

Table 3 Classes of L-methionine-responsive gene signatures and their top functions

ID	Molecules in network	Score	Focus	Top functions
1	**↓AURKA, ↓AURKB, ↓BIRC5, ↓BUB1, ↓CCNA2, ↓CCNB1, ↓CCNB2, ↓CDC2, ↓CDC20, ↓CDC25C, ↓CDCA8, ↓CENPA,** Cyclin B, Cyclin E, E2f, **↓E2F2**, ERK, **↓FBXO5, ↓FOXM1, ↓HMMR, ↓KIF14, ↓KIF23, ↓KIF4A, ↓KIFC1, ↑LAMA3, ↓MAD2L1, ↓NDC80, ↓PBK, ↓PRC1, ↓PRR11, ↓RACGAP1, ↓SPC25, ↓TK1, ↓TPX2, ↓TTK**	**74**	**31**	Cancer, cell cycle, reproductive system disease
2	Alcohol group acceptor phosphotransferase, **↓ASPM, ↓AURKB, ↓BUB1,** BUB1B, **↓CCNB2,** CCNG1, CDKN2A, **↓CENPE, ↓CEP55,** DSN1, E4F1, **↓FEN1,** Glutathione peroxidase, **↑GPX8, ↓HJURP, ↓HMGB2, ↓MELK,** NCAPD2, NCAPD3, **↓NCAPG2,** NCAPH2, **↓NDC80, ↓NEK2, ↓NUSAP1, ↓PRC1,** PRIM1, **↓RACGAP1, ↓TACC3,** TGFB1, **↓TK1,** TP53, **↓TTK,** UBE2A, **↓ZWINT (includes EG:11130)**	**41**	**21**	Cell cycle, cellular assembly and organization, DNA replication, recombination, and repair
3	Ap1, **↓ASF1B, ↑C8ORF4,** Caspase, **↓CDC45L,** Ck2, **↓CTSL2,** Cyclin A, **↓FEN1, ↓GMNN,** hCG, Histone h3, Histone h4, **↓KIAA0101,** Lamin b, **↓LMNB1, ↓LMNB2,** MAP2K1/2, **↓MCM2, ↓MCM3, ↓MCM7, ↓MCM10, ↑NQO1,** P38 MAPK, **↓PCNA,** Pka, Pkc(s), Rb, RNA polymerase II, RPA, **↓STMN1, ↓TIMELESS, ↓TOP2A, ↓UHRF1, ↓UNG**	**41**	**20**	DNA replication, recombination, and repair, cancer, gastrointestinal disease
4	ADAM15, **↑ATF3, ↓BUB1,** BYSL, CALCR, **↓CCNB2, ↓CDC20, ↓CDC45L, ↓CDKN3, ↓CNTNAP2,** CTR9, EGFR, HMGA2, IL6, **↓KIF11, ↓KIF2C,** KRT18, LCK, MAD2L2, MPDZ, **↓NMU, ↓NUDT1, ↓OIP5,** PDGF BB, **↓POLE2, ↓PSRC1,** PTPRK, SELENBP1, **↑SH3BGRL,** Tgf beta, **↓TK1, ↓TRIP13,** TRO, **↓TROAP**	**35**	**18**	Cancer, gastrointestinal disease, cell cycle
5	**↑AFF3,** AGA, **↓AIF1L, ↑AKR1C2,** C11ORF48, C15ORF15, C4ORF43, CASP3, **↓CDC45L, ↓CDCA3, ↓CDCA5, ↓CDCA7,** DDX27, DFFB, **↓DLGAP5,** EIF2S1, **↓GGH,** HBXIP, HNF4A, INCENP, IRS1, **↓KIF20A, ↓LMNB1, ↓LYAR,** MIRN210 (includes EG:406992), **↓MND1,** MYC, NAT10, Proteasome, PWP1, RAD51, **↑RBM4B,** TRAF2, **↑VAMP5, ↓WDR51A**	**30**	**16**	Cancer, gastrointestinal disease, genetic disorder
6	**↓FBXO38,** KLF7	**2**	**1**	Cell death, neurological disease, nervous system development and function

The genes were classified based on molecular networks (www.Ingenuity.com; see text). The downward arrows indicate genes that were down-regulated by L-methionine exposure in both LNCaP and MCF-7 cells, and the upward arrows indicate genes that were up-regulated in both cell lines. The expression of genes indicated without arrows and not in bold-face in these networks was unchanged in response to L-methionine treatment; the expression of four of these genes was changed in only one of the two cell lines (NCAPD3, UBE2A, ADAM15, and C4ORF43). Ingenuity Pathways Analysis computes a score for each network according to the fit of that network to the user-defined set of Focus Genes. This score is derived from a *P*-value and indicates the likelihood of the Focus Genes in a particular network being found together due to random chance. A score of 2 indicates that there is a 1 in 100 chance that the Focus Genes are together in a network due to random chance. Therefore, scores of 2 or higher have at least a 99% confidence of not being generated by random chance alone. This score is given in the third column of this table, and the number of focus genes that were changed in expression is given in the fourth column

A large number of genes that were down-regulated by L-methionine are members of protein kinase families. It is likely that many of these genes are associated with control of cell proliferation. Pathway analysis indicated down-regulation of a large number of genes involved in cancer, cell cycle, cell assembly and/or involved in organization, cell replication, recombination/repair of DNA, gastrointestinal disease, and genetic disorders by L-methionine treatment. This could be consistent with the inhibitory effects of L-methionine on LNCaP and MCF-7 cell growth (Benavides et al. 2007; Benavides et al. 2010). On the other hand, no effects in gene groups associated with methionine metabolism specifically were detected by pathway analysis. Nevertheless, the array data generated in this study form the basis of future studies with multiple methionine doses and time points comparing not only breast and prostate cancer cells, but also cancer cells with non-tumorigenic cells from the same tissues. This is particularly important in view of the fact that methionine only inhibits cell cycle progression in breast and prostate cancer cells but not in non-tumorigenic breast and prostate epithelial cells (Benavides et al. 2010). Although such future hypothesis generating studies would also provide sufficient data to develop and test models that explore how methionine may selectively affect cancer cells, they should also focus on generating experimental evidence that the observed changes in expression of the genes have functional significance. For example, the potential modifying effects of methionine on antioxidant mechanisms would be one fruitful area of future investigation.

In summary, this study indicates that L-methionine induces common changes in molecular signatures of MCF-7 breast cancer cells and LNCaP prostate cancer cells, down-regulating genes belonging to protein kinase families, which may be related to the anti-proliferative effects of this amino acid on these cells. L-methionine also up-regulated some genes involved in cellular redox regulation suggesting antioxidant activity–enhancing properties of this amino acid. Future studies of the mechanisms and consequences of cellular and molecular effects of L-methionine and development of methionine analogs that lack the potential negative effects of methionine itself on the well-known methionine-dependence of many tumor cells (Judde et al. 1989) may eventually lead to exploitation of analogs of this amino acid in cancer therapy.

Acknowledgments Supported in part by a Supplement to NIH Grant No. R01CA116195. The authors thank Dr Jin-Qiang Chen and Dr Daniel Guimaraes Tiezzi for technical and edition assistance.

Conflict of interest statement We declare that we have no conflict of interest.

References

Anderson ME (1998) Glutathione: an overview of biosynthesis and modulation. Chem Biol Interact 111–112:1–14

Bello RI, Gomez-Diaz C, Navarro F, Alcain FJ, Villalba JM (2001) Expression of NAD(P)H:quinone oxidoreductase 1 in HeLa cells: role of hydrogen peroxide and growth phase. J Biol Chem 276:44379–44384

Benavides MA, Oelschlager DK, Zhang HG, Stockard CR, Vital-Reyes VS, Katkoori VR, Manne U, Wang W, Bland KI, Grizzle WE (2007) Methionine inhibits cellular growth dependent on the p53 status of cells. Am J Surg 193:274–283

Benavides MA, Hagen KL, Fang W, Du P, Lin S, Moyer MP, Yang W, Bland KI, Grizzle WE, Bosland MC (2010) Suppression by L-methionine of cell cycle progression in LNCaP and MCF-7 cells but not benign cells. Anticancer Res (Accepted for publication)

Benjamini Y, Hochberg Y (1995) Controlling the false discovery rate: a practical and powerful approach to multiple testing. J Roy Statist Soc Ser B 57:289–300

Dalle-Donne I, Rossi R, Colombo G, Giustarini D, Milzani A (2009) Protein S-glutathionylation: a regulatory device from bacteria to humans. Trends Biochem Sci 34:85–96

Du P, Kibbe WA, Lin SM (2007) nuID: a universal naming scheme of oligonucleotides for illumina, affymetrix, and other microarrays. Biol Direct 2:16

Fagerholm R, Hofstetter B, Tommiska J, Aaltonen K, Vrtel R, Syrjakoski K, Kallioniemi A, Kilpivaara O, Mannermaa A, Kosma VM, Uusitupa M, Eskelinen M, Kataja V, Aittomaki K, von Smitten K, Heikkila P, Lukas J, Holli K, Bartkova J, Blomqvist C, Bartek J, Nevanlinna H (2008) NAD(P)H: quinone oxidoreductase 1 NQO1*2 genotype (P187S) is a strong prognostic and predictive factor in breast cancer. Nat Genet 40:844–853

Forthoffer N, Gomez-Diaz C, Bello RI, Buron MI, Martin SF, Rodriguez-Aguilera JC, Navas P, Villalba JM (2002) A novel plasma membrane quinone reductase and NAD(P)H: quinone oxidoreductase 1 are upregulated by serum withdrawal in human promyelocytic HL-60 cells. J Bioenerg Biomembr 34:209–219

Gallagher S (2001) Quantitation of nucleic acids with absorption spectroscopy. Curr Protoc Protein Sci (Appendix 4: Appendix 4K)

Giustarini D, Rossi R, Milzani A, Colombo R, Dalle-Donne I (2004) S-glutathionylation: from redox regulation of protein functions to human diseases. J Cell Mol Med 8:201–212

Horoszewicz JS, Leong SS, Kawinski E, Karr JP, Rosenthal H, Chu TM, Mirand EA, Murphy GP (1983) LNCaP model of human prostatic carcinoma. Cancer Res 43:1809–1818

Huang E, Ishida S, Pittman J, Dressman H, Bild A, Kloos M, D'Amico M, Pestell RG, West M, Nevins JR (2003) Gene expression phenotypic models that predict the activity of oncogenic pathways. Nat Genet 34:226–230

Ji Q, Chang L, VanDenBerg D, Stanczyk FZ, Stolz A (2003) Selective reduction of AKR1C2 in prostate cancer and its role in DHT metabolism. Prostate 54:275–289

Ji Q, Aoyama C, Nien YD, Liu PI, Chen PK, Chang L, Stanczyk FZ, Stolz A (2004) Selective loss of AKR1C1 and AKR1C2 in breast cancer and their potential effect on progesterone signaling. Cancer Res 64:7610–7617

Judde JG, Ellis M, Frost P (1989) Biochemical analysis of the role of transmethylation in the methionine dependence of tumor cells. Cancer Res 49:4859–4865

Lin SM, Du P, Huber W, Kibbe WA (2008) Model-based variance-stabilizing transformation for Illumina microarray data. Nucleic Acids Res 36:e11

Lou H, Du S, Ji Q, Stolz A (2006) Induction of AKR1C2 by phase II inducers: identification of a distal consensus antioxidant response element regulated by NRF2. Mol Pharmacol 69:1662–1672

Mazzocco M, Maffei M, Egeo A, Vergano A, Arrigo P, Di Lisi R, Ghiotto F, Scartezzini P (2002) The identification of a novel human homologue of the SH3 binding glutamic acid-rich (SH3BGR) gene establishes a new family of highly conserved small proteins related to thioredoxin superfamily. Gene 291:233–239

Metayer S, Seiliez I, Collin A, Duchene S, Mercier Y, Geraert PA, Tesseraud S (2008) Mechanisms through which sulfur amino acids control protein metabolism and oxidative status. J Nutr Biochem 19:207–215

Pratt SE, Pollak MN (1993) Estrogen and antiestrogen modulation of MCF7 human breast cancer cell proliferation is associated with specific alterations in accumulation of insulin-like growth factor-binding proteins in conditioned media. Cancer Res 53:5193–5198

SantaCruz KS, Yazlovitskaya E, Collins J, Johnson J, DeCarli C (2004) Regional NAD(P)H: quinone oxidoreductase activity in Alzheimer's disease. Neurobiol Aging 25:63–69

Shrivastava A, Nunn AD, Tweedle MF (2009) Designer peptides: learning from nature. Curr Pharm Des 15:675–681

Smyth G (2004) Linear models and empirical Bayes methods for assessing differential expression in microarray experiments. Stat Appl Genet Mol Biol (3: Article 3)

Sweet-Cordero A, Mukherjee S, Subramanian A, You H, Roix JJ, Ladd-Acosta C, Mesirov J, Golub TR, Jacks T (2005) An oncogenic KRAS2 expression signature identified by cross-species gene-expression analysis. Nat Genet 37:48–55

Takahashi K, Suzuki K (1993) Association of insulin-like growth-factor-I-induced DNA synthesis with phosphorylation and nuclear exclusion of p53 in human breast cancer MCF-7 cells. Int J Cancer 55:453–458

Thomas T, Thomas TJ (2001) Polyamines in cell growth and cell death: molecular mechanisms and therapeutic applications. Cell Mol Life Sci 58:244–258

Toppo S, Vanin S, Bosello V, Tosatto SC (2008) Evolutionary and structural insights into the multifaceted glutathione peroxidase (Gpx) superfamily. Antioxid Redox Signal 10:1501–1514

Vazquez E, Ferrer-Miralles N, Mangues R, Corchero JL, Schwartz S Jr, Villaverde A (2009) Modular protein engineering in emerging cancer therapies. Curr Pharm Des 15:893–916

Yin L, Xiang Y, Zhu DY, Yan N, Huang RH, Zhang Y, Wang DC (2005) Crystal structure of human SH3BGRL protein: the first structure of the human SH3BGR family representing a novel class of thioredoxin fold proteins. Proteins 61:213–216